

# Learning Control Applied to Electro-Hydraulic Poppet Valves

Patrick Opdenbosch, Nader Sadegh, Wayne Book

**Abstract**—This paper describes a novel state trajectory control method and its application to Electro-Hydraulic Poppet Valves (EHPV). The control objective is to find a control sequence that forces the state of the plant to asymptotically converge to the desired state trajectory. This is to be accomplished without requiring exact information about the state transition map of the plant. In fact, it is desired to learn the inverse input-state map of the plant at the same time that state tracking control is enforced. As an application of this novel controller, the tracking of a desired supply pressure trajectory is considered. This is achieved by learning the flow conductance coefficient  $K_v$  of the EHPV. The novel state trajectory control method achieves this objective by learning the inverse input-state mapping of the valve at the same time that this mapping is used in the feedforward loop. The mapping learning is accomplished with the aid of a simple neural network structure called the Nodal Link Perceptron Network (NLPN). The NLPN is trained online via a gradient descent method to minimize the errors in the inverse input-state mapping approximation. The supply pressure tracking performance subject to the proposed controller is validated through experimental data.

## I. INTRODUCTION

Controlling fluid power components, in particular electro-hydraulic valves, is not a straight forward task due to their inherent nonlinear characteristics [3,12]. For example, electro-hydraulic valves have a nonlinear pressure/flow relationship and exhibit hysteresis. Their performance is also affected by complex flow forces and friction [11].

The Electro-Hydraulic Poppet Valve (EHPV) considered in this paper is shown in Fig. 1 and described in [15,30,31]. This valve opens proportionally to the amount of current sent to its solenoid even though this relationship is nonlinear. Among the distinguishing features, this valve possesses an internal pressure compensation mechanism. This mechanism ensures that the minimum amount of current needed to initially open the valve is always consistent. Moreover, this valve has virtually ‘zero’ leakage, it is bidirectional, and has low hysteresis. The EHPV’s are typically used in a Wheatstone bridge arrangement for motion control of hydraulic actuators [26,27].

A simple approach, widely employed in industry to control complex systems, is to use a static look-up table (in some

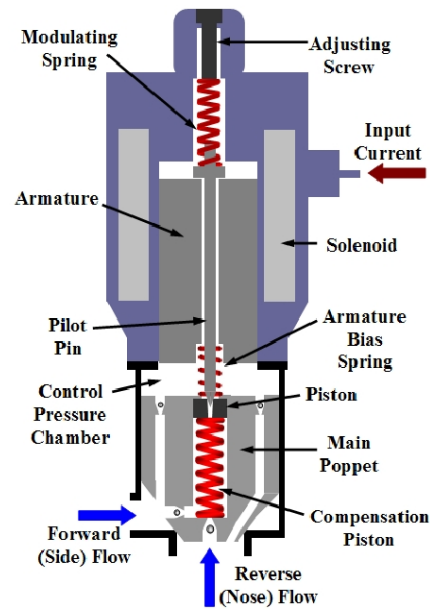


Fig. 1. Electro-Hydraulic Poppet Valve(EHPV) considered in this paper

cases adaptive [28]) with the inverse input-output characteristics of the plant in the feedforward path. In industry, the EHPV is currently controlled open-loop using this form of fixed calibration.

In an effort to present an alternative control approach, this paper applies a newly developed auto-calibration and control method to the EHPV. More specifically, the tracking of a desired supply pressure profile using the EHPV is considered herein. The control technique applied here is called *NLPN-based Input Matching* (NBIM) [13]. This technique simultaneously learns the inverse input-state mapping of the plant while forcing its state to follow a prescribed desired trajectory. The main requirements for the successful application of the control law presented here are knowledge of the order of the plant and some generic data to initialize the inverse mapping. This last requirement can be easily fulfilled by using steady-state data or equilibrium points of the plant.

Inverse Mapping Control (IMC), Adaptive Inverse Dynamics Control (AIDC), Input Matching (IM), Inverse Model Control, and Direct Learning Control are similar techniques that are useful for auto-calibration and control of complex systems. The concept of Input Matching was introduced by Johnson and Tse [6] and further developed by Goodwin et al. [4]. The AIDC method was developed in the early 80’s by Widrow and colleagues [29]. In the late 80’s, Psaltis et al. dis-

This work was supported in part by the Fluid Power Motion Control Center and HUSCO Intl.

P. Opdenbosch is a Ph.D. candidate in the George W. Woodruff School of Mechanical Engineering at the Georgia Institute of Technology, Atlanta GA, 30332, USA. patrick.opdenbosch@gatech.edu

N. Sadegh, Ph.D. is an associate professor in the George W. Woodruff School of Mechanical Engineering at the Georgia Institute of Technology, Atlanta GA, 30332, USA. nader.sadegh@me.gatech.edu

W. Book, Ph.D., is the HUSCO/Ramirez Distinguished Professor in Fluid Power and Motion Control in the George W. Woodruff School of Mechanical Engineering at the Georgia Institute of Technology, Atlanta GA, 30332, USA. wayne.book@me.gatech.edu

cussed the Direct Learning method for tracking control [19]. Malinowski et al. used the term Inverse Mapping Control to propose the use of static inverse mapping as controllers for time-invariant or slowly varying dynamic systems [10]. Pham and Oh in [16] used recurrent neural networks with backpropagation adaptation to approach the inverse dynamic control problem via input matching. In addition, Pham and Yildirim compared the performance of a SCARA robot under standard controllers, the Inverse Model Control, and Internal Model Control in [17]. It is concluded in this paper that the robot exhibited superior performance under the last two control schemes.

Advanced control techniques have also found their application in the field of fluid power technology. One finds the inclusion of feedforward learning compensation in addition to standard feedback control in [2,5,18,32]. Furthermore, a coordinated motion controller with learning capabilities was presented by Johnson et al. [5]. The learned inverse orifice characteristics were combined with PD control and a moderate improvement in performance was reported. Moreover, Song and Koivo in [25] used a feedforward multilayered neural network with backpropagation adaptation to model the inverse dynamics of an excavator. The offline training of the network utilized the input matching approach. While these researchers reported that the performance of the learning controller was superior to that of independent joint PID control, they acknowledged the slow convergence of this adaptation technique.

Recently, Liu and Yao in [9] proposed the online modeling of the flow mappings for unidirectional cartridge valves using neural networks. In this research, the valve flow mappings were considered static and the valve dynamics were neglected. The authors claim that the method has the advantage of calibrating the valves without removing them from the system. Similarly, Opdenbosch and Sadegh applied an adaptive NLPN-based control approach to the EHPV [14]. It was shown that the tracking performance of this valve was improved by using the adaptive NLPN-based controller.

It should be noted that most of the works found in the literature deal with output tracking error instead of state tracking error. In addition, it is seen in the literature that auto-calibration schemes can add value to the use of fluid power components. The contribution of this paper is the use of the NLPN<sup>1</sup> in the input matching technique, instead of using recurrent neural networks with backpropagation, and its application to control the EHPV by learning its *input-state* mapping.

The rest of the paper is organized as follows: the problem statement is presented in Section II along with relevant definitions and assumptions. The functional approximator that is used to accomplish the learning portion of the proposed methodology is introduced in Section III. After this, the control law is given in Section IV followed by its application to the EHPV in Section V. This section is followed by the

conclusions of the paper.

The following notations are freely used in this paper: The  $n$ -dimensional euclidean space is denoted by  $\mathbb{R}^n$  and the space of real  $m \times n$  matrices is denoted by  $\mathbb{R}^{m \times n}$ . A matrix is represented in bold while scalars and vectors are represented in normal fonts. For a given matrix  $\mathbf{B}$ , the  $i^{\text{th}}$  entry is represented by  $B_{ij}$  and the  $i^{\text{th}}$  column is denoted by  $[\mathbf{B}]_i$ . For a given vector  $x$ ,  $[x]_i$  denotes the  $i^{\text{th}}$  component. If  $x \in \mathbb{R}$ , then  $|x|$  denotes the absolute value of  $x$ , whereas if  $x \in \mathbb{R}^n$ , then  $|x|$  denotes the euclidean norm. The expression  $x = O(y)$  implies that  $x \rightarrow 0$  as  $y \rightarrow 0$  while the expression  $x = o(y)$  implies that  $x/y \rightarrow 0$  as  $y \rightarrow 0$ . The notation  $D_i^k f_j$  will be used to denote the  $k^{\text{th}}$  partial derivative of the  $j^{\text{th}}$  component of function  $f$  with respect to its  $i^{\text{th}}$  argument.

## II. PROBLEM STATEMENT

The system or plant to be controlled is assumed to have a discrete-time state space representation. As such, consider a general discrete-time nonlinear dynamic plant governed by the difference equation

$$\begin{aligned} x_{k+1} &= F(x_k, u_k) \\ x_{k_0} &= x_0 \end{aligned} \quad (1)$$

where the plant state is  $x_k \in \mathbb{R}^n$ , the input is  $u_k \in \mathbb{R}^n$ , and  $F : \mathbb{R}^n \times \mathbb{R}^n \rightarrow \mathbb{R}^n$  is the state transition map. Let the sampling time be fixed. The objective is to find a control sequence  $\{u_k\}_{k=k_0}^{\infty}$  that forces the state of the plant  $x_k$  to asymptotically converge to  $x_k^d$ , a given desired state trajectory. This is to be accomplished without requiring exact information about the state transition map  $F$  of the plant. In fact, it is desired to learn the inverse input-state map of the plant at the same time state tracking control is enforced.

**Remark 1** *When the plant is not in the form of (1), the Block Input-State approach [1,21] can be used to lift the dimension of the input vector to that of the state resulting in a square system.*

The following definitions are presented to formalize and clarify the understanding of some of the conventions employed herein. Note that in this paper,  $\bar{\mathcal{X}}$  and  $\bar{\mathcal{U}}$  denote the closure of the sets  $\mathcal{X}$  and  $\mathcal{U}$  respectively.

**Definition 1** *The set of admissible states, in which desired states are included, is denoted by  $\mathcal{X}$ . This set is a bounded and convex open subset of  $\mathbb{R}^n$ .*

**Definition 2** *The set of admissible inputs is denoted by  $\mathcal{U} := \{u \in \mathbb{R}^n : z = F(x, u), \text{ for some } x, z \in \mathcal{X}\}$ .*

**Definition 3** *The inverse input-state map of the plant in (1), when it exists, is denoted by  $u_k = \Psi(x_{k+1}, x_k)$ .*

**Definition 4** *The equilibrium or steady state inverse input-state map of the plant in (1) is denoted by  $u_{ss} = \Psi(x_{ss}, x_{ss})$  if it exists.*

<sup>1</sup>The Nodal Link Perceptron Network (NLPN) is in simple words an adaptive lookup table (see Section III).

**Definition 5** The NLPN input space is denoted by  $\mathcal{A}$ . When approximating the function  $\Psi$ , then  $\mathcal{A} = \bar{\mathcal{X}} \times \bar{\mathcal{X}}$ .

The control formulation presented herein is developed under the following set of assumptions. It is worth mentioning that other authors have used equivalent versions of these assumptions in the literature (see for example [7,8,24]).

**Assumption 1** The complete state vector  $x \in \mathbb{R}^n$  is feedback available.

**Assumption 2** The state transition map  $F : \mathbb{R}^n \times \mathbb{R}^n \rightarrow \mathbb{R}^n$  belongs to Class  $C^2$  (twice continuously differentiable) in the entire space  $\bar{\mathcal{X}} \times \bar{\mathcal{U}}$ .

**Assumption 3** The partial derivative of the state transition map  $D_2F(x, u)$  is nonsingular  $\forall x \in \bar{\mathcal{X}}$  and  $\forall u \in \bar{\mathcal{U}}$ .

**Assumption 4** For all  $x, z \in \mathcal{X}$ , there exists a unique vector  $u \in \mathbb{R}^n$  such that  $z = F(x, u)$ .

Assumption 3 ensures that the input-state map is locally invertible [24]. The last of these is often referred to as the *strong controllability* assumption in the literature [7,24]. In simple words, this assumption guarantees that any initial state in  $\mathcal{X}$  can be transferred to any final state in  $\mathcal{X}$  by means of a control sequence of length  $n$ .

It is important to mention that fulfillment of assumptions 2 through 4 implies the existence of a differentiable control function for the plant.

**Proposition 1** Consider the plant in (1) and suppose assumptions 2 through 4 are satisfied. Then, there exists a unique differentiable function  $\Psi : \mathcal{X} \times \mathcal{X} \rightarrow \mathcal{U}$  with the following properties: a) The admissible input set  $\mathcal{U}$  is nonempty, open, and bounded. b) For all  $x, z \in \mathcal{X}$  and  $u \in \mathcal{U}$ , then  $u = \Psi(z, x) \iff z = F(x, u)$ . Moreover,  $D_1\Psi = [D_2F]^{-1}$  and  $D_2\Psi = -[D_2F]^{-1}D_1F$ .

The proof of this proposition is a straightforward application of the Implicit Function Theorem and can be found in [13]. See [7,8,24] for similar results.

Another important assumption is that the mapping learning can be accomplished with the aid of an NLPN.

**Assumption 5** The inverse input-state map of the plant in (1) is in the functional space of the NLPN. In other words,  $\exists \mathbf{W} \in \mathbb{R}^{N \times n}$  and  $|\varepsilon_\Psi| \leq \varepsilon$  for some  $\varepsilon > 0$  such that  $\Psi = \mathbf{W}^T\Phi + \varepsilon_\Psi$ .

### III. FUNCTIONAL APPROXIMATOR

The learning part of the controller developed in this paper uses the Nodal Link Perceptron Network (NLPN). This perceptron-type neural network architecture is very similar to the Cerebellar Model Articulation Controller (CMAC) network and it was developed by Sadegh in [20,23]. The NLPN gives an attractive solution to the control problem since it is simple and compatible with existing look-up

tables found in many industrial control systems. The formal definition of the NLPN is given next.

**Definition 6** Let  $\mathcal{B}_N = \{\phi_i\}_{i=1}^N$  be a finite set of basis functions. A  $\mathcal{B}_N$  based NLPN is referred to as a three-layered perceptron network whose hidden layer consists of  $N$  activation functions  $\phi_1, \phi_2, \dots, \phi_N \in \mathcal{B}_N$  with the following input-output relationship:

$$f_w(x) = \sum_{i=1}^N [\mathbf{W}^T]_i \phi_i(x) = \mathbf{W}^T \Phi(x)$$

where  $x \in \mathcal{A}$  and  $f_w \in \mathbb{R}^m$  are the input and output vectors of the network, and  $[\mathbf{W}]_i \in \mathbb{R}^N$  (i.e.  $\mathbf{W} \in \mathbb{R}^{N \times m}$ ) is the vector of nodal weights.  $\Phi(x)$  is the basis function vector whose  $i^{\text{th}}$  entry is  $[\Phi(x)]_i = \phi_i(x)$ .

Even though other choices are available, piece-wise linear basis functions are used in this paper because of their simplicity. As such, consider the case in which  $x \in \mathbb{R}^n$ . Without loss of generality, it is assumed that the input space is reshaped so that  $\mathcal{A} = [\alpha_1, \beta_1] \times \dots \times [\alpha_n, \beta_n]$  and each interval is divided into  $N_j$  subintervals  $[\lambda_{i,j}, \lambda_{i+1,j}]$  with  $\alpha_j = \lambda_{1,j} < \lambda_{2,j} < \dots < \lambda_{N_j,j} < \lambda_{N_j+1,j} = \beta_j$ . This way, the input space  $\mathcal{A}$  is partitioned into  $N_c = \prod_{j=1}^n N_j$  rectangular cubes. The corners of these cubes are referred to as the *nodal points* of  $\mathcal{A}$ . The total number of nodal points is  $N_A = \prod_{j=1}^n (N_j + 1)$ . Now, the output of a *piece-wise linear* basis function is computed from

$$\begin{aligned} \phi_{i \in \mathcal{I}}(x) &= \prod_{j=1}^n \varphi_{i,j}(x_j) \\ \varphi_{m,j}(x_j) &= \begin{cases} \frac{(x_j - \lambda_{m-1,j})}{(\lambda_{m,j} - \lambda_{m-1,j})} & \text{if } x_j \in [\lambda_{m-1,j}, \lambda_{m,j}] \\ \frac{(\lambda_{m+1,j} - x_j)}{(\lambda_{m,j} - \lambda_{m+1,j})} & \text{if } x_j \in [\lambda_{m,j}, \lambda_{m+1,j}] \\ 0 & \text{else} \end{cases} \end{aligned} \quad (2)$$

where  $\mathcal{I}$  is a countable index set.

**Example 1** Consider the case for  $x \in \mathbb{R}^2$  and assume that the two dimensional input space is given by  $\mathcal{A} = [0, 1] \times [-5, 5]$ . The first interval for this space is divided into a single ( $N_1 = 1$ ) subinterval. The second interval is divided into  $N_2 = 2$  subintervals. In other words,

$$\begin{aligned} [\lambda_{1,1} \quad \lambda_{2,1}] &= [0 \quad 1] \\ [\lambda_{1,2} \quad \lambda_{2,2} \quad \lambda_{3,2}] &= [-5 \quad 0 \quad 5] \end{aligned}$$

It can be seen from Figure 2 that there are two rectangular cubes and six nodal points. Now, consider the index set

$$\mathcal{I} = \{(1, 1), (1, 2), (1, 3), (2, 1), (2, 2), (2, 3)\}$$

Then, for example, the output of the basis functions for the index (1, 2) is given by

$$\phi_{(1,2)}(x) = \varphi_{1,1}(x_1) \varphi_{2,2}(x_2)$$

Now, the vector of basis functions is formed as

$$\Phi(x) = [\phi_{(1,1)} \quad \phi_{(2,1)} \quad \dots \quad \phi_{(1,3)} \quad \phi_{(2,3)}]^T$$

This vector is then combined with a set of weights to produce the output of the NLPN.



**Theorem 1** Consider the discrete-time system in (1) subject to the control law (5) using the steepest descent adaptation (4). Assume that  $\gamma_k$  is chosen such that  $0 \leq \gamma_k |\Phi(x_k, x_{k-1})|^2 < 2$  and that assumptions 1 through 4 are satisfied. If the state sequence  $x_k$  is Persistently Exciting, then there exist positive scalars  $\bar{k}_p < 1$ ,  $\bar{e}_0$ ,  $\bar{e}_{\hat{\Psi}}$ , and  $\varepsilon$  such that if  $|1 - K_p| \leq \bar{k}_p$ ,  $|e_0| \leq \bar{e}_0$ ,  $|\Psi - \hat{\Psi}_0|_A \leq \bar{e}_{\hat{\Psi}}$ , and  $\varepsilon_{\Psi} \leq \varepsilon$ , then  $e_k$  and  $u_k$  are bounded for all  $k$ . Moreover,  $\lim_{k \rightarrow \infty} \sup |e_k| = O(\varepsilon)$  and  $\lim_{k \rightarrow \infty} |\Psi - \hat{\Psi}|_A \leq O(\varepsilon)$ .

*Proof:* The proof of this theorem is too long to be included here. The reader can find it in [13]. A simple example is given next for illustration purposes. ■

**Example 2** Consider a scalar linear time invariant plant whose state equation is given by  $x_{k+1} = Ax_k + Bu_k$ . Assume that the plant is controllable. Let the state tracking error be given by  $e_k := x_k^d - x_k$ . It is not difficult to see that the true inverse input-state mapping of this plant is given by  $u_k = \Psi(v_1, v_2) = B^{-1}(v_1 - Av_2)$ . If this mapping is known exactly, then substitution of the control law

$$u_k = \Psi(x_{k+1}^d, x_k^d) - K_p [D_2 \Psi(x_{k+1}^d, x_k^d)] e_k$$

into the plant state dynamics yields  $e_{k+1} = (1 - K_p) Ae_k$ . The resulting error dynamics is stable provided that the feedback gain is chosen to satisfy  $\frac{|A|-1}{|A|} < K_p < \frac{|A|+1}{|A|}$ .

**Remark 3** Theorem 1 asserts that the tracking error and the inverse mapping approximation error will be in the order of the capabilities of the NLPN. It is required that the initial state tracking error be small and that there exists an initial input-state mapping. This mapping is used to initialize  $\hat{W}$ . In practice, this last requirement can be easily fulfilled by using steady-state data or equilibrium points of the plant.

## V. APPLICATION TO HYDRAULICS

As mentioned before, the opening (conductance) of each EHPV is currently controlled by open-loop means. A fixed look-up table is populated with the valve's inverse input-output relationship<sup>3</sup> obtained from steady state data. This is accomplished by recording the relationship between the current sent to the solenoid (input) and the valve's flow conductance coefficient  $Kv$  (output). This calibration is performed for both flow directions (bidirectionality). Because of slow time varying characteristics (wear and tear, temperature effects, etc), the EHPV's would require periodic recalibrations for optimal performance. At this point, the valves are not recalibrated online (*i.e.* while they are in operation).

There are three major advantages of using a learning controller for the EHPV: *first*, there would be no need to obtain extensive individual calibrations for valves of the same size. With the learning controller, generic data can be used and the discrepancies are corrected online. *Second*, the EHPV's performance can be improved by combining

<sup>3</sup>Referred to as the valve calibration hereafter.

feedback control. *Third*, by knowing how the EHPV is truly behaving while in operation, a maintenance schedule can be implemented from monitoring and detecting the deviations from the normal pattern of behavior<sup>4</sup>.

It is the experience of the authors that this valve can also be controlled by combining nonlearning feedforward compensation (look-up table based on steady state data) and standard PID feedback control. However, this type of controller would be more sensitive to errors in the feedforward compensation. Also, the third advantage introduced by the learning controller is not matched by the PID-based control scheme.

As described in Section IV, the order of the EHPV and some generic or initial data about the inverse input-state mapping are needed to successfully apply the control law. This is explored next.

The generic data is extracted from the steady state characteristics of the EHPV, briefly described next. Typical steady state data for the EHPV are presented in Fig. 4. This plot shows the relationship between  $Kv$ , the pressure differential across the valve  $\Delta P$ , and the input current sent to the solenoid. Note that temperature effects are neglected herein. It is important to notice that the flow conductance is nearly independent of the pressure differential for  $\Delta P$  values greater than 0.4 MPa. This feature will be exploited to simplify the control task.

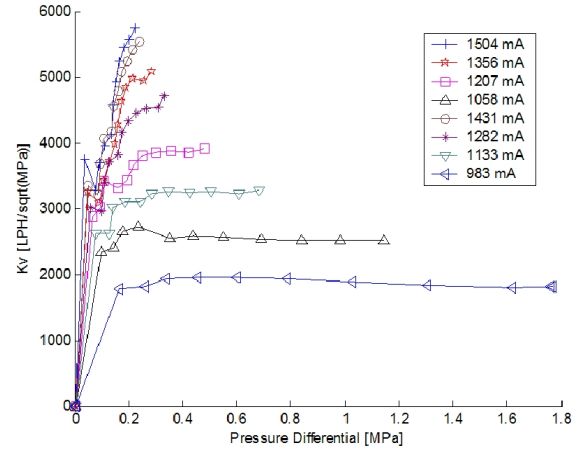


Fig. 4. Steady state data for the forward flow direction of the EHPV

The step response of the EHPV to different input currents is shown in Fig. 5<sup>5</sup>. The data appears considerably noisy for higher current values because the pressure differential decreased as the valve opened more. Consequently, pressure signals became more noisy. In this paper, the flow conductance  $Kv$  is obtained from

$$Kv = Q/\sqrt{\Delta P}$$

by measuring the flow through the valve and the pressure differential.

<sup>4</sup>This health monitoring aspect will be explored in a future paper.

<sup>5</sup>Note that the three different step inputs were not applied at the same time.

The step responses from a model of the EHPV are shown in red in Fig. 5. This model is composed of a linear second order system with a static input nonlinearity [13]. This static nonlinearity is realized with the data shown in Fig. 4. It is important to mention that it is not necessary to have a model of the EHPV for the successful application of the control law. This is done to give insight and make the case for the order of the EHPV. From looking at Fig. 5, one can take a step further and argue that the valve has first order dynamics (*i.e.* a single state). With this consideration, the EHPV is automatically in the desired form of (1). Consequently, the flow conductance of the EHPV is approximated herein by

$$Kv_{k+1} = F(Kv_k, u_k)$$

where  $u_k$  is the current sent to the solenoid.

To test the control law, the EHPV labeled 'SR' is used to control the supply pressure  $P_S$  in the hydraulic circuit depicted in Fig. 6. This pressure is labeled as such since it is the supply pressure for the Wheatstone bridge arrangement of EHPV's. In this hydraulic test-bed, all the pressures, the position, and the velocity of the piston are available via CAN bus.

A simple pressure control scheme that uses the valve's  $Kv$  is described next. A desired flow conductance  $Kv^d$  is commanded for the 'SR' valve. The  $Kv^d$  value is computed from the desired supply pressure  $P_S^d$  by

$$Kv^d = \frac{Q_p(P_S^d) - \dot{x}A}{\sqrt{P_S^d - P_R}} \quad (6)$$

where  $Q_p(\cdot)$  is the supply flow from the pump given in Fig. 7 and  $A$  is the appropriate area of the piston. The actual flow conductance of the valve is computed using (6) with the actual pressure  $P_S$ .

The response of the EHPV subject to the control law is evaluated next. The resulting performance when the learning is disabled is presented first. This is seen in Fig. 8 and 9.

The response of the valve in terms of tracking the desired flow conductance is given in Fig. 8 when the learning is

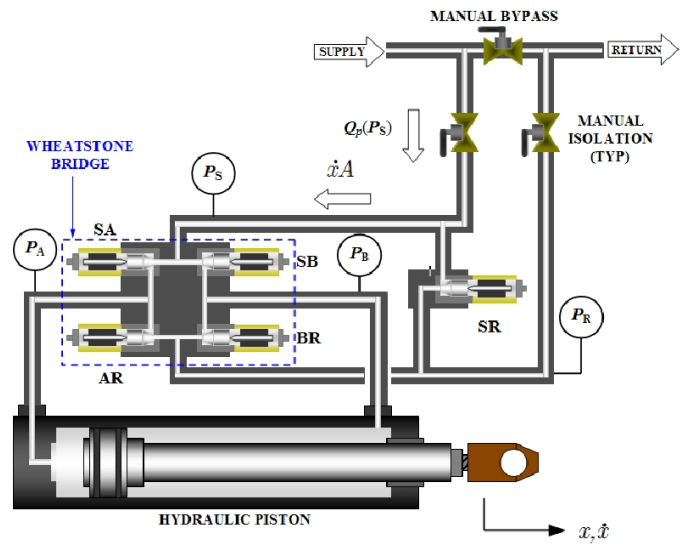


Fig. 6. Hydraulic test-bed used in the pressure control application

disabled. In this figure, 'KSRc' represents the commanded or desired  $Kv$  while 'KSRm' denotes the measured one. The tracking performance of the resulting supply pressure is depicted in Fig. 9. In this figure, the desired supply pressure or setpoint pressure, manually commanded, is labeled 'Psp' while the other signals are measured.

When the adaptation is enabled, the resulting  $Kv$  response is given in Fig. 10. In addition, the resulting performance of the supply pressure is presented in Fig. 11. The superior performance of the learning method is clearly identified. However, some oscillations are observed in the pressure response shown in Fig. 11. This could be further improved by taking into account fluid inertance and fluid compressibility, neglected in the control law of (6).

The settings of the control law are discussed next. The input space of the NLPN is to be fed with the pair  $(Kv_k, Kv_{k-1})$  according to 3. However, it was anticipated that most of the data would remain close to the line  $Kv_k =$

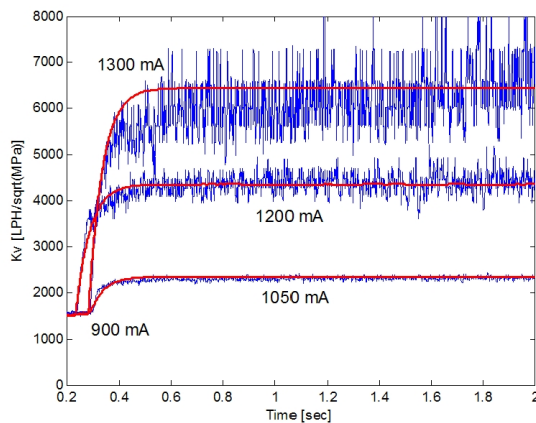


Fig. 5. Step response of the EHPV under different input currents

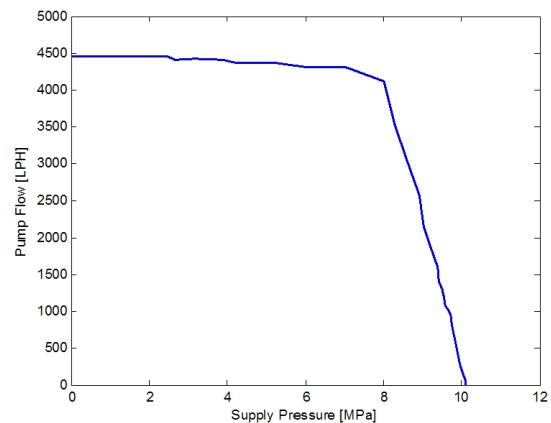


Fig. 7. Supply flow from the pump as a function of  $P_S$

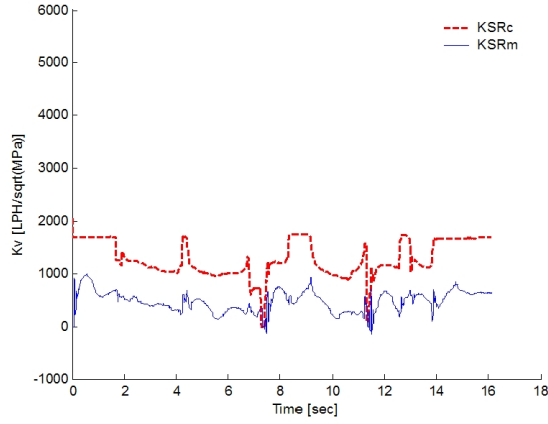


Fig. 8. Flow conductance response without learning

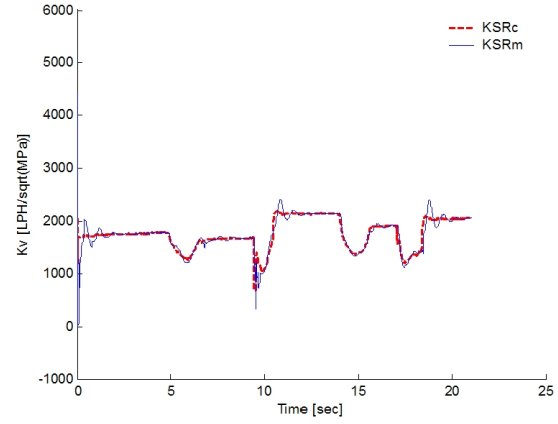


Fig. 10. Flow conductance response with learning

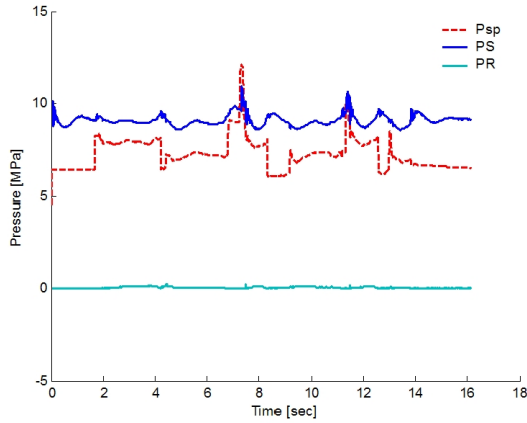


Fig. 9. Supply pressure response without learning

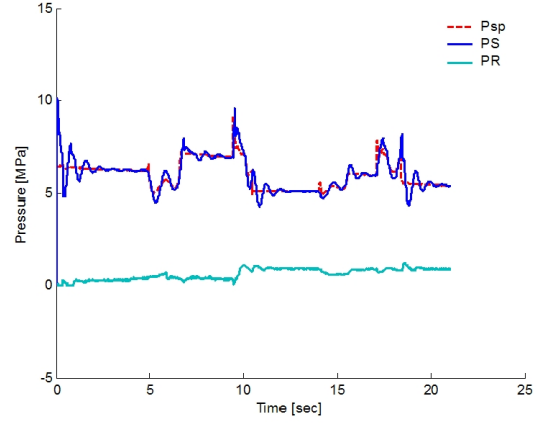


Fig. 11. Supply pressure response with learning

$Kv_{k-1}$ , the *steady state* line. Consequently, a coordinate transformation is used to rotate (a  $45^\circ$  rotation) the input space to align the  $Kv_k$  axis with the steady state line. This way, the node distribution along this axis can be determined offline from trends seen in the steady state data. The new axes are labeled  $z_1$  and  $z_2$ , where  $z_1 = \sqrt{2}(Kv_k + Kv_{k-1})/2$  and  $z_2 = \sqrt{2}(Kv_{k-1} - Kv_k)/2$ . The input space is partitioned as  $\mathcal{A} = g_1 \times g_2$ , where the grid vectors are expressed in  $\text{LPH}/\sqrt{\text{MPa}}$  by

$$\begin{aligned} g_1 &= [-100, 15, 310, 330, 500, 1000, 12000] \\ g_2 &= [-4000, -500, 0, 500, 4000] \end{aligned}$$

The learning rate  $\gamma$  was set to 0.2 while the proportional gain  $K_p$  was set to 0.1. These values were manually tuned and could be further changed by compromising adaptation speed and relative stability if desired. The term  $D_2\Phi$  was computed by differentiating (2). At the nodal points, where  $\Phi$  is not differentiable, the derivative is computed by setting it to the value it had before coming to the nodal point.

Notice that the pressure across the valve was always maintained *high enough* (above 2 MPa). This was done to take

advantage of the  $Kv$  independence from  $\Delta P$ . Consequently, the initial inverse input-state mapping can be obtained from slicing the data shown in Fig. 4 at a constant  $\Delta P$  and inverting it. Note that the initial calibration used herein, shown in Fig. 12, was degraded on purpose from the true calibration to show the capabilities of the control law. This figure also shows the learned inverse input-state (labeled as final) and a typical extensive calibration curve for this valve size. In addition, notice that the learned curve starts at about 800 mA as opposed to the others. This is because this region in the input space of the NLPN was seldom visited as seen in Fig. 10. Hence, it was affected but not correctly learned. Notice that the desired  $Kv$  remained mostly between 1000 and 2000  $\text{LPH}/\sqrt{\text{MPa}}$ , and thus very good agreement is seen between the learned and the extensively calibrated curve in this region.

## VI. CONCLUSIONS

This paper presented the application of an online auto-calibration and control method for the EHPV. More specifically, the tracking of a desired supply pressure profile using the EHPV was considered. The control law presented herein

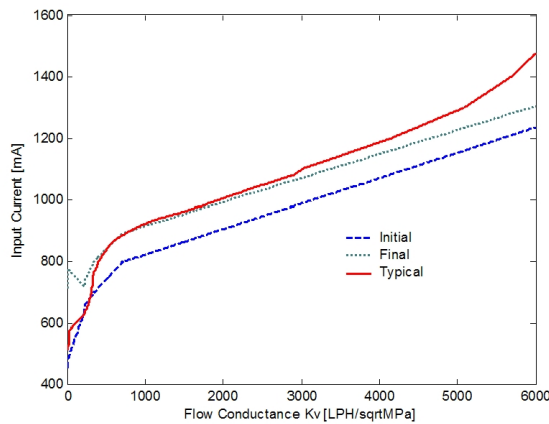


Fig. 12. Inverse input-state mappings for the EHPV at steady state

simultaneously learned the inverse input-state mapping of the EHPV while forcing its flow conductance to follow a prescribed desired trajectory. This was accomplished by treating the EHPV as nonlinear plant with first order dynamics and using an initial input-state mapping obtained from steady state data. Consequently, the controlled pressure showed good tracking capabilities as opposed to simply using an open-loop static look-up table based controller. Although not shown here, the performance of the EHPV under open-loop control (based on the extensive calibration mapping) showed good steady state performance but poor tracking due to the open-loop dynamics of the valve.

## VII. ACKNOWLEDGMENTS

The authors gratefully acknowledge the support provided to this project by HUSCO International and the Fluid Power Motion Control Center at Georgia Tech.

## REFERENCES

- [1] P. Albertos, "Block multirate input-output model for sampled-data control systems," *IEEE Transactions on Automatic Control*, vol. 35, no. 9, pp. 1085–1088, 1990.
- [2] J. E. Bobrow and K. Lum, "Adaptive, high bandwidth control of a hydraulic actuator," *Transactions of the ASME. Journal of Dynamic Systems, Measurement and Control*, vol. 118, no. 4, pp. 714–720, 1996.
- [3] K. A. Edge, "The control of fluid power systems - responding to the challenges," *Proceedings of the Institution of Mechanical Engineers*, vol. 211 Part I, no. 2, pp. 91–110, 1997.
- [4] G. C. Goodwin, J. Johnson, C. R., and S. Kwai Sang, "Global convergence for adaptive one-step-ahead optimal controllers based on input matching," *IEEE Transactions on Automatic Control*, vol. AC-26, no. 6, pp. 1269–73, 1981.
- [5] D. W. Johnson, I. Lovell, G. H., and J. J. Murray, "Development of a coordinated motion controller for a front shovel excavator," ser. *Proceedings of the ANS Seventh Topical Meeting on Robotics and Remote Systems*, vol. 1, 1997, pp. 239–46.
- [6] J. Johnson, C. R. and E. Tse, "Adaptive implementation of one-step-ahead optimal control via input matching," ser. *Proceedings of the IEEE Conference on Decision and Control*, 1977, pp. 145–50.
- [7] A. U. Levin and K. S. Narendra, "Control of nonlinear dynamical systems using neural networks: controllability and stabilization," *IEEE Transactions on Neural Networks*, vol. 4, no. 2, pp. 192–206, 1993.
- [8] —, "Control of nonlinear dynamical systems using neural networks - part ii: observability, identification, and control," *IEEE Transactions on Neural Networks*, vol. 7, no. 1, pp. 30–42, 1996.

- [9] S. Liu and B. Yao, "On-board system identification of systems with unknown input nonlinearity and system parameters," ser. *ASME Dynamic Systems and Control Division*, vol. 74, 2005, pp. 1079–1085.
- [10] A. Malinowski, J. M. Zurada, and J. H. Lilly, "Inverse control of nonlinear systems using neural network observer and inverse mapping approach," ser. *IEEE International Conference on Neural Networks - Conference Proceedings*, vol. 5, 1995, pp. 2513–2518.
- [11] D. McCloy and H. R. Martin, *Control of fluid power: analysis and design*, 2nd ed. New York: John Wiley and Sons, 1980.
- [12] H. E. Merritt, *Hydraulic control systems*. New York: John Wiley and Sons Inc, 1967.
- [13] P. Opdenbosch, "Auto-calibration and control applied to electro-hydraulic valves," Ph.D. Dissertation, Georgia Institute of Technology, 2007.
- [14] P. Opdenbosch and N. Sadegh, "Control of electro-hydraulic poppet valves via online learning and estimation," ser. *ASME The Fluid Power and Systems Technology Division*, vol. 12, 2005, pp. 57–62.
- [15] P. Opdenbosch, N. Sadegh, and W. J. Book, "Modeling and control of an electro-hydraulic poppet valve," ser. *ASME The Fluid Power and Systems Technology Division*, vol. 11, 2004, pp. 103–110.
- [16] D. T. Pham and S. J. Oh, "Adaptive control of dynamic systems using neural networks," in *International Conference on Systems, Man and Cybernetics. Systems Engineering in the Service of Humans*, vol. 4, 1993, pp. 97–102.
- [17] D. T. Pham and S. Yildirim, "Comparison of four methods of robot trajectory control," in *15th Triennial World Congress on Automatic Control*, 2002.
- [18] U. Pinsopon, T. Hwang, S. Cetinkunt, R. Ingram, Q. Zhang, M. Cobo, D. Koehler, and R. Ottman, "Hydraulic actuator control with open-centre electrohydraulic valve using a cerebellar model articulation controller neural network algorithm," *Journal of Systems and Control Engineering*, vol. 213, no. 1, pp. 33–48, 1999.
- [19] D. Psaltis, A. Sideris, and A. A. Yamamura, "A multilayered neural network controller," *IEEE Control Systems Magazine*, vol. 8, no. 2, pp. 17–21, 1988.
- [20] N. Sadegh, "A multilayer nodal link perceptron network with least squares training algorithm," *International Journal of Control*, vol. 70, no. 3, pp. 385–404, 1998.
- [21] N. Sadegh and B. Maqueira, "Output control of discrete-time nonlinear systems," ser. *Proceedings of the American Control Conference*, vol. 2, 1994, pp. 2175–2179.
- [22] N. Sadegh, "Nonlinear identification and control via neural networks," in *Winter Annual Meeting of the American Society of Mechanical Engineers*, vol. 33, 1991, pp. 46–56.
- [23] —, "A nodal link perceptron network with applications to control of a nonholonomic system," *IEEE Transactions on Neural Networks*, vol. 6, no. 6, pp. 1516–1523, 1995.
- [24] —, "Trajectory learning and output feedback control of nonlinear discrete-time systems," ser. *40th IEEE Conference on Decision and Control*, vol. 4, 2001, pp. 4032–4037.
- [25] B. Song and A. J. Koivo, "Neural adaptive control of excavators," ser. *Proceedings of the IEEE/RSJ International Conference on Intelligent Robots and Systems*, vol. 1, 1995, pp. 162–7.
- [26] K. A. Tabor, "Velocity based method for controlling a hydraulic system," U.S. Patent 6,718,759, April, 2004.
- [27] —, "A novel method of controlling a hydraulic actuator with four valve independent metering using load feedback," in *SAE Commercial Vehicle Engineering Congress and Exhibition*, 2005.
- [28] M. Vogt, N. Muller, and R. Isermann, "On-line adaptation of grid-based look-up tables using a fast linear regression technique," *Transactions of the ASME. Journal of Dynamic Systems, Measurement and Control*, vol. 126, no. 4, pp. 732–739, 2004.
- [29] B. Widrow, D. Shur, and S. Shaffer, "On adaptive inverse control," ser. *Fifteenth Asilomar Conference on Circuits, Systems and Computers*, 1982, pp. 185–9.
- [30] X. Yang, "Pilot solenoid control valve with pressure responsive diaphragm," U.S. Patent 6,149,124, November, 2000.
- [31] X. Yang, J. L. Pfaff, and M. J. Paik, "Pilot operated control valve having a poppet with integral pressure compensating mechanism," U.S. Patent 6,745,992, June, 2004.
- [32] D. Zheng, H. Havlicsek, and A. Alleyne, "Nonlinear adaptive learning for electrohydraulic control systems," ser. *ASME The Fluid Power and Systems Technology Division*, vol. 5, 1998, pp. 83–90.